Nanoscale Advances

ROYAL SOCIETY OF CHEMISTRY

PAPER

View Article Online
View Journal | View Issue

Cite this: *Nanoscale Adv.*, 2020, **2**, 2507

Dispersion of high-quality boron nitride nanosheets in polyethylene for nanocomposites of superior thermal transport properties

Zhengdong Wang,[a] Paul Priego,[a] Mohammed J. Meziani,*[b] Kathleen Wirth,[a] Sriparna Bhattacharya,[c] Apparao Rao,*[c] Ping Wang[a] and Ya-Ping Sun*[a]

Received 6th March 2020
Accepted 8th April 2020

DOI: 10.1039/d0na00190b

rsc.li/nanoscale-advances

High-quality boron nitride nanosheets (BNNs) characterized by large aspect ratios and less defective surfaces and structures are in demand for thermal management and other uses that exploit the uniquely advantageous properties of boron nitride, such as being highly thermally conductive yet electrically insulating and extreme chemical and thermal stabilities. In this study, an ammonia-assisted exfoliation processing method was developed and applied to the preparation of high-quality BNNs. As a demonstration of the excellent potential of these nanomaterials, the BNNs were dispersed in polyethylene polymers for nanocomposite films of superior thermal transport performance at levels significantly beyond the state of the art in the literature. Effects of crosslinking in the nanocomposite film structure on thermal transport were also explored and favorable outcomes were achieved.

Introduction

The production and use of high-quality boron nitride nanosheets (BNNs) have attracted much recent attention.[1,2] Unlike their graphene counterparts, BNNs are thermally conductive yet electrically insulating, and in addition they are known for their excellent chemical and thermal stabilities and strong resistance to oxidation even at elevated temperatures.[1–4] Most BNNs are prepared from hexagonal boron nitride (h-BN) by using various exfoliation methods, similar in principle and practice to the exfoliation of graphite into few-layer graphene nanosheets. However, the stronger inter-layer interactions in h-BN, commonly referred to as "lip–lip" interactions, which are associated with the slightly ionic bonding characteristics between neighboring B and N both in plane and out of plane, make exfoliation into high-quality BNNs significantly more difficult than peeling off graphene from graphite. Here, "high quality" generally refers to nanosheets that are thinner and also larger in lateral dimensions, thus a higher aspect ratio, and also fewer defects in the structure and on the surface. A number of exfoliation approaches and associated processing conditions have been pursued, from simple sonication in a preferred solvent like isopropanol to the use of strong mechanical force in ball-milling,[5–9] and they are all driven by the perceived need for supplying sufficient energy externally to enable exfoliation. However, the energy supplied in many of the exfoliation methods may break h-BN into nanoscale pieces, but often not BNNs of the desired high quality for highly thermally conductive polymeric nanocomposites. In fact, since BNNs produced by a simple exfoliation method of sonication in isopropanol could achieve relatively high thermal conductive performance in their corresponding nanocomposites,[7] one may argue that relatively "gentler" exfoliation approaches and processing conditions for less defective BNNs can be advantageous in their thermal transport related applications. It has been shown that amino molecules due to their binding to electron deficient boron sites[10] could be used to enhance the exfoliation of h-BN in solvent dispersions.[3,9,11] For such a purpose, smaller molecules are generally preferred for being able to penetrate the inter-layer spacing to aid the desired exfoliation. Thus, in this work ammonia as the smallest amino molecule was used, coupled with vigorous sonication in the preferred solvent isopropanol, to produce targeted high-quality BNNs in stable solvent suspensions.

The dispersion of BNNs in polymeric matrices, namely the detailed structural arrangements between the fillers and matrix polymers in nanocomposites, must be equally important to the observed thermal transport performance. This may explain, to some extent, the obviously significant variations in experimentally determined thermal conductivity values for the same or similar BNNs in different polymer matrices. Specifically for polyethylene (PE) composites, most investigations have been on the use of boron nitride (BN) without deliberate exfoliation as the filler. For example, Zhang *et al.* extruded polyethylene with BN for somewhat oriented composites with a thermal

[a]*Department of Chemistry and Laboratory for Emerging Materials and Technology, Clemson University, Clemson, South Carolina 29634, USA. E-mail: syaping@clemson.edu*

[b]*Department of Natural Sciences, Northwest Missouri State University, Maryville, Missouri 64468, USA. E-mail: meziani@nwmissouri.edu*

[c]*Department of Physics and Astronomy, Clemson Nanomaterials Institute, Clemson University, Clemson, South Carolina 29634, USA. E-mail: arao@clemson.edu*

conductivity of up to 3.6 W mK^{-1} at a 40 wt% BN loading.[12] Huang, *et al.* applied the solid-phase extrusion method to the fabrication of polyethylene composites with h-BN at loadings of 30 vol% and 50 vol%, corresponding to the observed thermal conductivity values of 8.6 W mK^{-1} and 12.4 W mK^{-1}, respectively.[13] These results suggest the generally poorer thermal transport performance of PE composites in comparison with other polymers, such as epoxy and poly(vinyl alcohol) polymers,[1,7] which is rather disappointing due to the fact that PE as an excellent commodity polymer is extensively used across a number of industries and also in many consumer products. In addition, while most PE samples are low in thermal conductivity, more crystalline PE materials or configurations, such as well-aligned nanofibers and nanowire arrays, have exhibited high thermal conductivity values.[14,15] Thus, potential effects on the crystallinity of matrix PE polymers due to the embedding of BNNs and the structural arrangements between the fillers and polymers in the nanocomposites are also interesting issues due to their relationship with the observed thermal transport properties. With the preparation of high-quality BNNs, their more homogeneous dispersion in the PE polymer matrix may represent a major opportunity in the development of highly thermally conductive PE/BNN nanocomposites, as successfully explored in the work reported here. Issues and opportunities for further performance improvements are discussed.

Experimental section

Materials

The hexagonal boron nitride (h-BN) sample (99.5%) and benzil (98%) were purchased from Alfa Aesar, aqueous ammonia solution (~28%) and isopropanol (99%) from Fisher Scientific, and *trans*-decalin (98%) from Beantown Chemical. Polyethylene was sourced from sandwich bags manufactured and marketed by S. C. Johnson & Son, Inc. Polyvinylidene fluoride (PVDF) membrane filters were acquired from Fisher Scientific, and carbon- and holey carbon-coated copper grids for electron microscopy analyses from SPI Supplies. Water was deionized and purified by being passed through a Labconco WaterPros water purification system.

Measurements

X-ray powder diffraction measurements were carried out on a Scintag XDS-2000 powder diffraction system. Scanning electron microscopy (SEM) imaging was performed on a JOEL JSM7600F field-emission scanning electron microscope (FE-SEM). A thin gold coating was applied to the electrically insulating boron nitride samples to mitigate any charging effect in SEM. Transmission electron microscopy (TEM) images were acquired on a Hitachi HD-2000 scanning-TEM system and Hitachi H-9500 TEM system, with the specimens on carbon- or holey carbon-coated copper grids. In the preparation of specimens for cross-sectional TEM analyses, a sample was embedded in epoxy resin, followed by microtoming with the use of a Reichert-Jung Ultracut E Microtome with a 30° angle diamond knife at room temperature for slices of less than 100 nm in thickness.

The in-plane thermal diffusivity in thin films (30–50 microns) was determined on an Ulvac LaserPIT thermal diffusivity/conductivity meter operated at room temperature in a vacuum of 0.01 Pa. The film specimen was about 30 mm × 5 mm in size, with one surface (facing the laser in the instrument) coated with a thin layer of graphite. At least three frequencies were used in the measurement of each film sample, and the readings were averaged for the specific specimen. The densities and specific heats of the nanocomposite films were estimated from those of the polymer and filler in terms of the simple mixing rule:

$$\text{composite} = w_{\text{polymer}}\text{polymer} + w_{\text{filler}}\text{filler},$$

where w denotes weight fractions.

Exfoliation

The as-supplied h-BN sample (1 g) in a mixture of aqueous ammonia solution (~28%) and isopropanol (3/2 v/v, 125 mL) was sonicated (VWR-250D, 120 W) for 48 h. The resulting suspension was centrifuged at 3000*g* to collect the supernatant. Upon vacuum filtration (0.45 micron Nylon EZFlow membrane filter) and then removal of the solvent, a solid sample of BNNs was obtained and used for characterization and the preparation of polymeric nanocomposites.

Nanocomposite films

Polyethylene (PE, 70 mg) was added to decalin and stirred at 95 °C overnight. The resulting solution was concentrated to obtain a PE polymer blend, which was cast onto a preheated (95 °C) etched glass slide. Upon solvent evaporation, a neat PE thin film could be peeled off the slide to be free-standing, and then the film was further dried in a vacuum oven at ~60 °C before its use as a blank in characterization and measurements.

For PE/BNN nanocomposite films, the BNN sample (200 mg) obtained from the exfoliation was dispersed in isopropanol (20 mL) *via* sonication for 30 min. Separately, a hot (95 °C) solution of PE in decalin was prepared. The solution was mixed with the BNN dispersion in various volume ratios, and the mixtures were stirred and sonicated at 65 °C. Upon concentration of the mixtures *via* solvent removal, the resulting blends were cast onto preheated glass slides. The free-standing PE/BNN nanocomposite films were obtained in the same way as the PE blank film described above.

The same protocol was applied in the preparation of PE/h-BN composite films, in which the as-supplied h-BN sample was used in place of BNNs.

Crosslinked PE/BNN nanocomposite films

In the protocol described above, benzil at a level of 3.5 mg per film was included in the solution before it was concentrated into a polymer blend. The resulting nanocomposite films containing benzil were peeled off the glass slides to be free-standing and then cured by exposure to ultraviolet light

(Spectroline high intensity ultraviolet lamp, 120 V and 1.05 A) for 5 h. Then, the films were further dried in a vacuum oven at 60 °C.

Results and discussion

In a recent study,[9] a series of exfoliation approaches coupled with different sets of processing conditions were evaluated systematically for the purpose of preparing high-quality BNNs. Among the more favorable approaches, exfoliation based on the use of aqueous ammonia mixed with isopropanol was thus identified and adopted in this study. Experimentally, the commercially supplied h-BN sample in the aqueous ammonia – isopropanol mixture was vigorously sonicated. The resulting suspension was centrifuged, and the supernatant was collected for vacuum filtration to remove small BN pieces and all solvent and other molecules. The filter cake was dried to obtain BNNs as a solid sample for characterization.

In the X-ray powder diffraction characterization, results of the precursor h-BN sample were used as the reference. The diffraction peaks of h-BN were at 2θ of 26.8°, 41.7°, 43.9°, 50.2°, and 55.2°, corresponding to the (002) ($d = 0.33$ nm), (100) ($d = 0.22$ nm), (101), (102), and (004) ($d = 0.16$ nm) planes, respectively. For the BNNs, the diffraction peaks corresponding to the (100), (101), (102), and (004) planes were weak and broader (Fig. 1), consistent with the sample containing mostly thin BNNs. The structural changes from the precursor h-BN to the exfoliated sample were reflected by the features of the (002) peak, which for the BNNs was at 2θ of 26.6°, about 0.2° lower than that of the precursor h-BN, and significantly broader (Fig. 1). The (002) and (004) peaks of the BNNs were also of relatively higher intensities, consistent with the expected preferential exfoliation along the (002) and/or (004) planes. With the Scherrer equation,[16] the broadening in X-ray diffraction peaks was used to estimate the average thickness of the BNNs as 10 ± 0.4 nm, with the variations reflecting the inhomogeneity in thickness distributions and lateral dimensions of the nanosheets.

The thickness of BNNs was determined directly by transmission electron microscopy (TEM). The TEM specimens were prepared by embedding the selected BNN sample in epoxy resin, followed by microtoming for ultrathin slices of less than 100 nm in thickness. The TEM images for a cross-sectional view of the nanosheets are shown in Fig. 2. The observed lattice fringes for the (002) planes allow the determination of a spacing of 0.334 nm. For average thickness, a limitation of TEM at such a high resolution is the inclusion of only a few nanosheets in an image. Thus, many images covering different areas of the TEM specimens to include about 40 nanosheets were used for statistical analyses (Fig. 2 inset), yielding an average thickness of 8.3 ± 2.8 nm, not far from the estimate based on the Scherrer equation. The TEM images also suggest that morphologically the BNNs retain clear lattice structures and have no major defects, supporting the notion that the use of ammonia in the processing can achieve effective exfoliation without any significant damages to the boron nitride 2D structures.[9]

The labeling of the ammonia-assisted exfoliation as a gentler approach is also supported by results from the SEM characterization of the thus produced BNNs. As shown in Fig. 3, the SEM images suggest that the nanosheets generally have smooth surfaces and edges and are less defective with lateral dimensions in the micron range. However, it should be pointed out that there is no practical metric even at a semi-quantitative level to measure the "defectiveness" (and the quality for that matter) of BNNs due to impossible experimental/technical limitations.

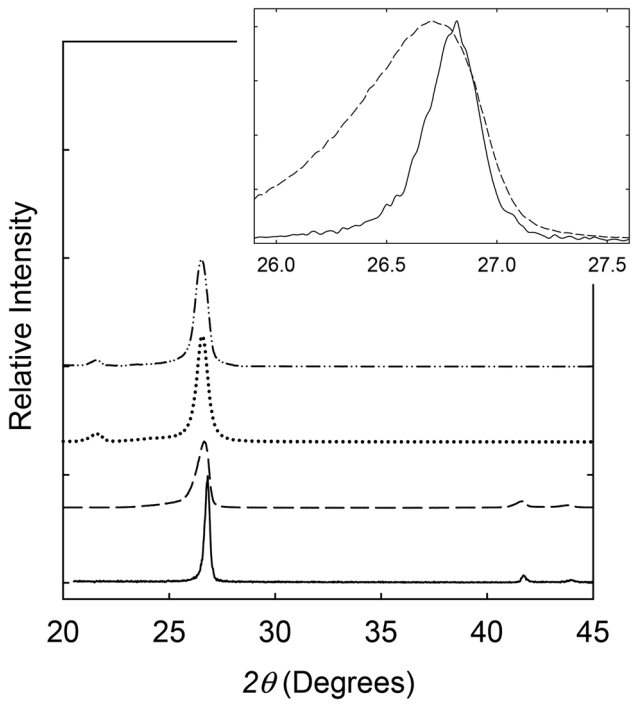

Fig. 1 X-ray diffraction patterns of the h-BN (solid line) and BNN (dashed line) samples, with the corresponding enlarged (002) peaks in the inset, and also PE/BNN (dotted line) and crosslinked PE/BNN (dash-dot-dot line) films.

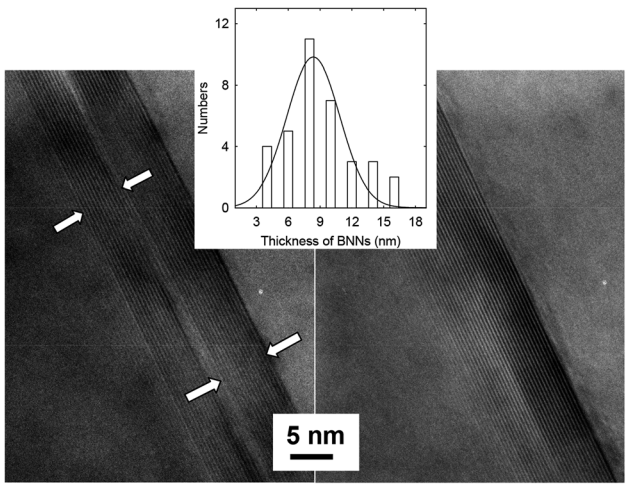

Fig. 2 TEM images for cross-sectional views of BNNs in the thin slices from microtoming. Inset: the thickness distribution analysis based on multiple TEM images.

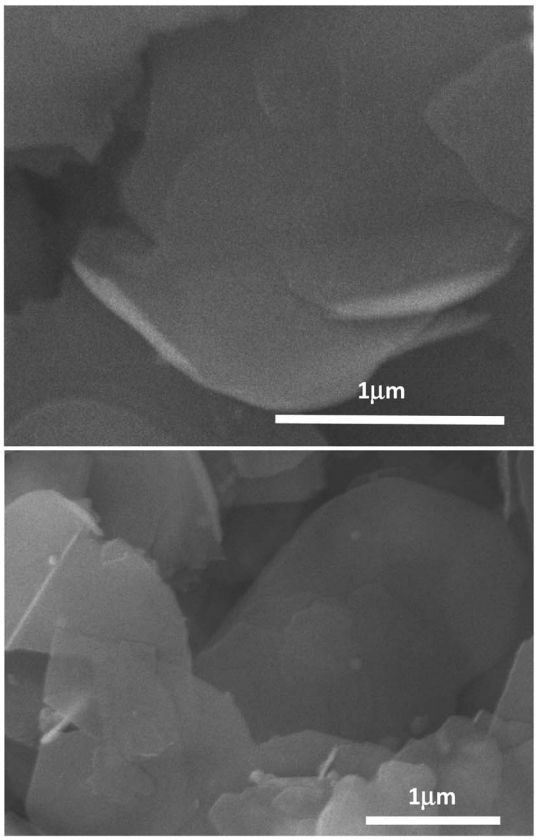

Fig. 3 SEM images for the BNN sample. The horizontal lines are scale bars with their represented lengths indicated in μm.

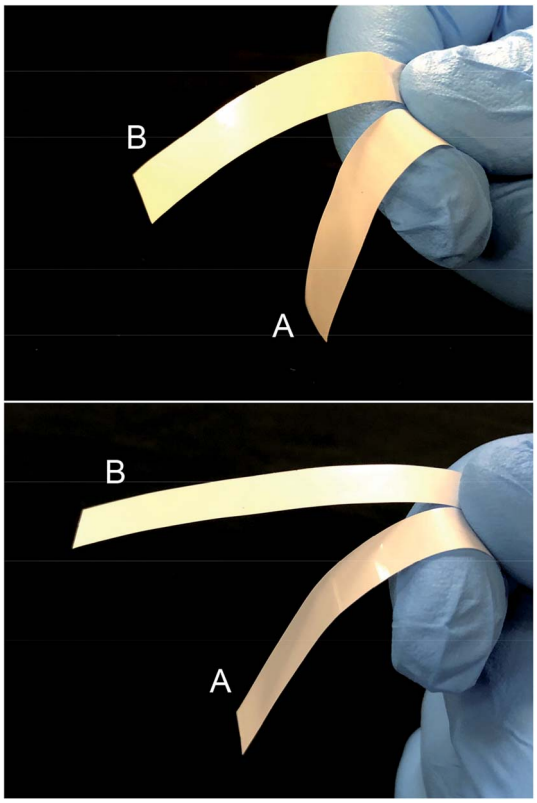

Fig. 4 Photos of PE/BNN (A) and crosslinked PE/BNN (B) films with 10 wt% (upper) and 30 wt% (lower) BNN loadings.

For the dispersion of BNNs in the polyethylene (PE) polymer matrix, the exfoliated sample in an isopropanol suspension was mixed well with a solution of PE polymers. Upon concentration, the resulting blend was used for PE/BNN nanocomposite films *via* wet-casting. After complete removal of solvents, all the free-standing films with different BNN loadings appeared smooth and flexible (Fig. 4). The films were characterized by X-ray diffraction analyses, with the results compared with those of the as-exfoliated BNN sample in Fig. 1. The characteristic diffraction peak for the (002) plane was only slightly shifted, 26.56° in the films *versus* 26.62° for free BNNs (Fig. 1), suggesting a minor increase in the average interlayer spacing due probably to the role of PE polymers. The absence of the (100) and (101) peaks at higher angles should be consistent with the preferential dispersion and orientation of BNNs along the (002) planes in the polymer film matrix. The average thickness of the BNNs estimated by the Scherrer equation was largely unchanged after their dispersion in PE polymers.

The thermal transport properties of the PE/BNN nanocomposite films were evaluated in terms of in-plane thermal diffusivity (TD) measurements on a commercially acquired instrument based on the modified Angstrom's method.[17,18] The TD is correlated with thermal conductivity (TC) in the following relationship:

$$\mathrm{TC} = \rho C_{\mathrm{p}} \mathrm{TD} \quad (1)$$

where ρ and C_{p} are the mass density and specific heat of the material, respectively. As shown in Table 1 and Fig. 5, the TC values are dependent on the BNN loadings in the nanocomposite films, increasing monotonically. On comparison between BNNs and h-BN as fillers, the films with the former generally have significantly higher TC values, validating the widely held understanding that nanosheets are more favorable fillers for polymeric nanocomposite films of higher thermal transport performance.[1] Also for comparison, at a BNN loading of 40 wt% in the PE/BNN nanocomposite film, the experimentally determined TD value (18 $\mathrm{mm^2\ s^{-1}}$, Table 1) is much higher than those obtained previously in polymeric epoxy/BNN and other nanocomposite films.[1,7] The substantial performance enhancement must be credited predominantly to the higher quality of the BNNs produced from the ammonia-assisted exfoliation, despite some expected effects and variations between different polymer film matrices.[9]

As compared in Fig. 5, the TC values of the nanocomposite films obtained in this work, including those of the PE/h-BN films, are generally higher than those of similar PE/BN composites reported in the literature (with sources provided and methods highlighted in the figure caption). To eliminate any potential artifacts or interference in the TD measurements, standard specimens of known TD values were used to calibrate the instrument and experimental protocols, and the calibration results were excellent. The performance advantages of the PE/h-BN films in this work over those reported in the literature might

Table 1 Thermal transport properties of PE nanocomposite thin films with h-BN and BNNs as fillers

Filler loading (wt%)	PE/h-BN		PE/BNNs		Crosslinked PE/BNNs	
	TD ($mm^2 s^{-1}$)	TC ($W mK^{-1}$)	TD ($mm^2 s^{-1}$)	TC ($W mK^{-1}$)	TD ($mm^2 s^{-1}$)	TC ($W mK^{-1}$)
0			0.2	0.46		
5			0.5	1.2		
7.5			1.3	3		
10	1.2	2.8	1.8	4.1	2.8	6.4
15			2.5	5.8	4	9.2
20	2.3	5.3	3.6	8.3	8.7	20
25			5.8	13	7.5	17
30	4.5	10	11	25	13	30
40			18	41		

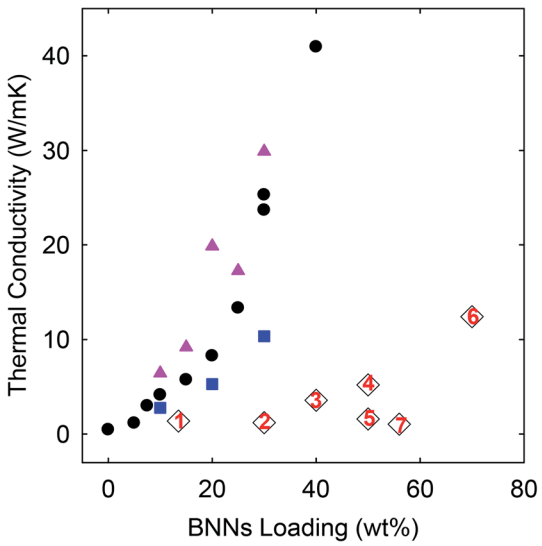

Fig. 5 TC results of the PE/h-BN (square), PE/BNN (circle), and crosslinked PE/BNN (triangle) films compared with those of similar films reported in the literature (1: ref. 19; 2: ref. 20; 3: ref. 12; 4: ref. 21; 5: ref. 22; 6: ref. 13; and 7: ref. 23).

be attributed in part to the filler dispersion characteristics in the films, as a more homogenous dispersion is known to be more favorable to thermal transport in the composite films. In fact, the effect of the film structural characteristics on thermal transport properties is clearly reflected by the improved TD/TC performance of the purposely crosslinked PE/BNN nanocomposite films.

For the crosslinking, benzil as a commonly employed photoinitiator was added to the mixture of the suspended BNNs and PE solution,resulting in the blend and the PE/BNN nanocomposite films. The films containing benzil were photoirradiated under a UV lamp for being cured and crosslinked. The X-ray diffraction results of the PE/BNN nanocomposite films with and without the crosslinking are largely the same (Fig. 1). The crosslinked films were similarly evaluated for thermal transport properties. The observed TD values are consistently higher than those of the corresponding films without the crosslinking, as compared in Table 1 and Fig. 5. It seems that the performance enhancement with the crosslinking is more pronounced at lower BNN loadings, about 50% improvement in the films of 10 wt% BNNs *versus* about 20% improvement in those with 30 wt% BNNs (Table 1), though a more systematic and comprehensive investigation is needed for a more definite conclusion. Nevertheless, the available results do suggest that the crosslinking, which likely makes the film structure more condensed and thus mechanically less flexible (Fig. 4), can generally improve the thermal transport performance of the PE/BNN nanocomposite films.

For microscopic/nanoscopic probing of the PE/BNN nanocomposite films, fractured edges were created by mechanically ripping apart the films and also by breaking the films after they were soaked in liquid nitrogen.The results from SEM imaging analyses of the fractured edges are shown in Fig. 6. The results are generally supportive of the expectation that the BNNs are well dispersed in the PE polymer matrix. The fractured edges of the nanocomposite films are much rougher than those of neat PE films, probably due to the dispersion of BNNs throughout the PE polymer matrix. In a closer examination, some BNNs could be found protruding out of the fractured edges across almost the entire cross-section, aligned parallel to the film surface. The patterns of tear marks from the mechanical ripping seem consistent with the presence of strong interactions between BNNs and their surrounding PE polymer chains in the nanocomposites, indicating that the BNNs of large aspect ratios and a relatively smooth surface as fillers may enable or facilitate the polymer chains to stretch and pack along the filler surface in the nanocomposite films. Such a microscopic/nanoscopic structural configuration, which is affected or dictated by the filler characteristics, must be correlated with the properties of the nanocomposite films.

The observed superior thermal transport performance of the PE/BNN nanocomposite films could be credited primarily to the high quality of the filler BNNs, including large aspect ratios and being less defective in the nanosheets. Due to these favorable characteristics, the ammonia-assisted exfoliation represents a relatively gentler yet effective processing method for high-quality BNNs.[9] The good dispersion of the fillers in the PE polymer matrix may also contribute to the performance, as reflected by the observed higher thermal conductivities with the use of h-BN without exfoliation than similar composites reported in the literature (Fig. 5). The significant improvements in

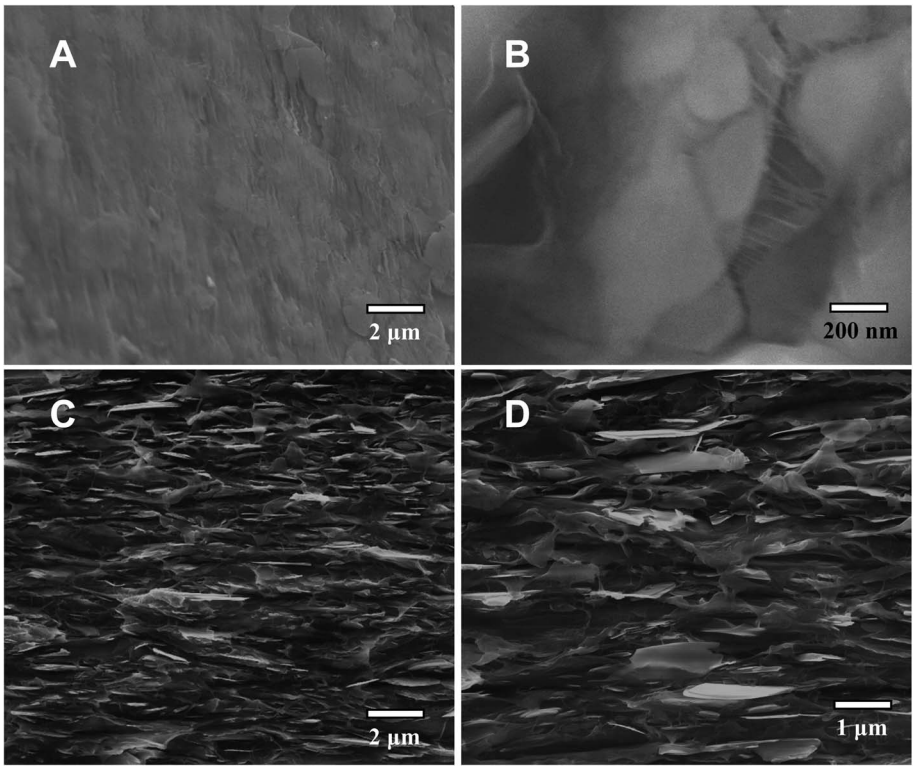

Fig. 6 SEM images for the crosslinked PE/BNN film with a 30 wt% BNN loading. (A) The film surface; (B) the fractured edge from mechanically ripping apart the film; and (C & D) fractured cross-sections from breaking the film at liquid nitrogen temperature.

thermal transport with the crosslinking in the PE/BNN nanocomposite films suggest that the microscopic/nanoscopic structures in the films, including probably the local densities, also play a meaningful role in the thermal transport. Mechanistically, the thermal conductivity is associated with phonon transport (vibrational progression), for which filler percolation may be a factor or even necessary, but hardly a sufficient condition.[1,24] This is very different from the electrical conductivity in similar nanocomposites with electrically conductive fillers (graphenes or carbon nanotubes, for example), and also makes the development of highly thermally conductive polymeric nanocomposites considerably more challenging. For desired nanocomposites of high thermal conductivity, high-quality fillers are obviously critical, but so are their "appropriate arrangements" in the nanocomposites. An understanding of the latter and the related parameterization still represent a tough task for experimental and theoretical investigations.

In conclusion, the ammonia-assisted exfoliation of h-BN has been found to represent a relatively gentler processing method for the production of high-quality BNNs,[9] which are characterized by large aspect ratios and fewer defects in the nanosheets and a relatively smooth nanosheet surface. There seem to be no major barriers in scaling up the exfoliation method for larger quantities of the BNNs. The dispersion of the high-quality BNNs in PE polymers resulted in nanocomposite films of superior thermal transport performance significantly beyond the state of the art in the literature. The exfoliation method may be further developed for BNNs of even more desirable characteristics and in large quantities for valuable applications across several technological fields.

Conflicts of interest

There are no conflicts to declare.

Acknowledgements

Financial support from NASA (80NSSC18M0033) is gratefully acknowledged. K. W. was a participant of Palmetto Academy, a summer undergraduate research program of the South Carolina Space Grant Consortium.

References

1 M. J. Meziani, W.-L. Song, P. Wang, F. Lu, Z. Hou, A. Anderson, H. Maimaiti and Y.-P. Sun, *ChemPhysChem*, 2015, **16**, 1339–1346.
2 D. V. Shtansky, K. L. Firestein and D. V. Golberg, *Nanoscale*, 2018, **10**, 17477–17493.
3 Y. Lin and J. W. Connell, *Nanoscale*, 2012, **4**, 6908–6939.
4 D. Golberg, Y. Bando, Y. Huang, T. Terao, M. Mitome, C. Tang and C. Zhi, *ACS Nano*, 2010, **4**, 2979–2993.
5 J. N. Coleman, M. Lotya, A. O'Neill, S. D. Bergin, P. J. King, U. Khan, K. Young, A. Gaucher, S. De, R. J. Smith, I. V. Shvets, S. K. Arora, G. Stanton, H.-Y. Kim, K. Lee,

G. T. Kim, G. S. Duesberg, T. Hallam, J. J. Boland, J. J. Wang, J. F. Donegan, J. C. Grunlan, G. Moriarty, A. Shmelev, R. J. Nicholls, J. M. Perkins, E. M. Grieveson, K. Theuwissen, D. W. McComb, P. D. Nellist and V. Nicolosi, *Science*, 2011, **331**, 568–571.

6 L. H. Li, Y. Chen, G. Behan, H. Zhang, M. Petravic and A. M. Glushenkov, *J. Mater. Chem.*, 2011, **21**, 11862–11866.

7 W.-L. Song, P. Wang, L. Cao, A. Anderson, M. J. Meziani, A. J. Farr and Y.-P. Sun, *Angew. Chem., Int. Ed.*, 2012, **51**, 6498–6501.

8 D. Deepika, L. H. Li, A. M. Glushenkov, S. K. Hait, P. Hodgson and Y. Chen, *Sci. Rep.*, 2014, **4**, 7288.

9 Z. Wang, M. J. Meziani, A. K. Patel, P. Priego, K. Wirth, P. Wang and Y.-P. Sun, *Ind. Eng. Chem. Res.*, 2019, **58**, 18644–18653.

10 S.-Y. Xie, W. Wang, K. A. S. Fernando, X. Wang, Y. Lin and Y.-P. Sun, *Chem. Commun.*, 2005, 3670–3672.

11 Y. Lin, T. V. Williams, W. Cao, H. E. Elsayed-Ali and J. W. Connell, *J. Phys. Chem. C*, 2010, **114**, 17434–17439.

12 X. Zhang, J. Zhang, L. Xia, C. Li, J. Wang, F. Xu, X. Zhang, H. Wu and S. Guo, *ACS Appl. Mater. Interfaces*, 2017, **9**, 22977–22984.

13 Y.-F. Huang, Z.-G. Wang, H.-M. Yin, J.-Z. Xu, Y. Chen, J. Lei, L. Zhu, F. Gong and Z.-M. Li, *ACS Appl. Nano Mater.*, 2018, **1**, 3312–3320.

14 S. Shen, A. Henry, J. Tong, R. Zheng and G. Chen, *Nat. Nanotechnol.*, 2010, **5**, 251–255.

15 V. Singh, T. L. Bougher, A. Weathers, Y. Cai, K. Bi, M. T. Pettes, S. A. McMenamin, W. Lv, D. P. Resler, T. R. Gattuso, D. H. Altman, K. H. Sandhage, L. Shi, A. Henry and B. A. Cola, *Nat. Nanotechnol.*, 2014, **9**, 384–390.

16 P. Scherrer, *Nachr. Ges. Wiss. Göttingen*, 1918, **26**, 98–100.

17 J. M. Belling and J. Unsworth, *Rev. Sci. Instrum.*, 1987, **58**, 997.

18 W. N. dos Santos, J. N. dos Santos, P. Mummery and A. Wallwork, *Polym. Test.*, 2010, **29**, 107–112.

19 S.-Y. Yang, Y.-F. Huang, J. Lei, L. Zhu and Z.-M. Li, *Composites, Part A*, 2018, **107**, 135–143.

20 X. Zhang, L. Shen, H. Wu and S. Guo, *Compos. Sci. Technol.*, 2013, **89**, 24–28.

21 Z.-G. Wang, F. Gong, W.-C. Yu, Y.-F. Huang, L. Zhu, L. Jun, J.-Z. Xu and Z.-M. Li, *Compos. Sci. Technol.*, 2018, **162**, 7–13.

22 P.-G. Ren, H. Si-Yu, R. Fang, Z. Zeng-Ping, S. Zhen-Feng and X. Ling, *Composites, Part A*, 2016, **90**, 13–21.

23 W. Zhou, S. Qi, H. Li and S. Shao, *Thermochim. Acta*, 2007, **452**, 36–42.

24 W.-L. Song, L. M. Veca, A. Anderson, M.-S. Cao, L. Cao and Y.-P. Sun, *Nanotech. Rev.*, 2012, **1**, 363–376.